Australian Government

Department of Defence

Defence Science and

Technology Organisation

An Accumulated Damage Model for Blast Propagation in Compartmented Structures with Progressively Failing Thin Bulkheads

L. K. Antanovskii

Weapons Systems Division

Defence Science and Technology Organisation

DSTO–TR–2365

ABSTRACT

This report addresses the development of a model for blast propagation in compartmented structures with progressively failing thin structural elements like windows. The mathematical model is based on the assumption that the frangible structural features (a) are thin compared to the characteristic length scale, (b) do not deform much before breakage, and (c) fail instantaneously when the corresponding accumulated damage reaches some threshold. The presented numerical model employs a variation of the Godunov scheme for blast propagation, coupled with a simple governing equation for the accumulated damage of finite elements constituting a structural feature with empirical coefficients estimated from the pressure-impulse diagram. When the accumulated damage exceeds some threshold value, a group of finite elements representing a designated entity like a single window, is forced to fail thus instantaneously changing the computational domain topology. The illustrative numerical simulations in three dimensions demonstrate that the model behaves reasonably well and is capable of providing rough estimates of progressive failure and blast transfer within and between compartmented structures.

APPROVED FOR PUBLIC RELEASE

APPROVED FOR PUBLIC RELEASE

An Accumulated Damage Model for Blast Propagation in Compartmented Structures with Progressively Failing Thin Bulkheads

Executive Summary

This report addresses the development of a model for blast propagation in compartmented structures with progressively failing thin structural elements like windows. The mathematical model is based on the assumption that the frangible structural features (a) are thin compared to the characteristic length scale, (b) do not deform much before breakage, and (c) fail instantaneously when the corresponding accumulated damage reaches some threshold. The presented numerical model employs a variation of the Godunov scheme for blast propagation, coupled with a simple governing equation for the accumulated damage of finite elements constituting a structural feature with empirical coefficients estimated from the pressure-impulse diagram. When the accumulated damage exceeds some threshold value, a group of finite elements representing a designated entity like a single window, is forced to fail thus instantaneously changing the computational domain topology. The illustrative numerical simulations in three dimensions demonstrate that the model behaves reasonably well and is capable of providing rough estimates of progressive failure and blast transfer within and between compartmented structures and hence provides useful input to blast effects vulnerability & lethality assessment codes.

The concept of accumulated damage can be equally applied to vulnerable components placed inside a structure. The component's accumulated damage normalised by its critical damage can be regarded as the probability of failure of the component. This approach replaces the notion of failure probability, which is very hard to measure and thus difficult to validate the corresponding model, with a conceptually simpler notion of accumulated damage governed by a dynamic equation.

The work has been performed under the National Security task NS 07/002.

Author

Leonid Antanovskii
Weapons Systems Division

Leonid Antanovskii obtained an MSc Degree with Distinction in Mechanics and Applied Mathematics from the Novosibirsk State University, Russia, and a PhD in Mechanics of Fluid, Gas and Plasma from the Lavrentyev Institute of Hydrodynamics, Russian Academy of Sciences. Since graduation he worked in academia and private industry for several research organisations and software development companies in Russia, Italy, Trinidad & Tobago, USA and Australia, being mostly involved in the modelling of various physical phenomena in fluid & solid mechanics. He joined DSTO in February 2007 where his current research interests include development of vulnerability & lethality models for weapon–target interaction.

Contents

1   Introduction

Interaction of blast waves with structures attracts the interest of many scientists and engineers [Bangash 1993, Jones & Brebbia 2006]. In many circumstances the most important question concerns the estimation of blast loads on the structure whose structural analysis is done after solving the gas dynamics problem in the known flow domain. This analysis is particularly important for structural engineers dealing with protecting critical infrastructure from the explosive events [Rose & Smith 2002, Smith & Rose 2002, Zhou, Hao & Deeks 2005, Remennikov & Rose 2005, Smith & Rose 2006, Remennikov & Rose 2007, Cluttera, Mathis & Stahl 2007].

In other practically important problems it is necessary to account for significant deformation of structures interacting with blast waves. In this case the governing equations of gas dynamics are coupled with those of solid mechanics through dynamically changing flow domain that becomes part of solution [Dowell & Hall 2001, Gong & Andreopoulos 2009]. When internal structural elements are fragile and have relatively little strength and mass, such as conventional glazing elements, the effects of their deformation before breakage and of the debris on the flow field can be neglected. In other words, when pressure load due to blast damages internal bulkheads and windows, the solution domain changes instantaneously and shock waves start propagating into adjacent compartments, potentially causing damage to other structural elements. The delay of breakage of internal structural elements results in a more complex flow pattern due to reflected shock waves. The flow pattern appears to be very sensitive to the time of failure which is quite difficult to predict without experiments.

The standard approach for estimation of the lifetime of structural elements is based on the pressure-impulse (P-I) diagram commonly used in the preliminary design of protective structures to establish safe response limits for given blast-loading scenarios [Baker 1973, Baker et al. 1983, Lloyd 1998, Gelfand & Silnikov 2004, Fallah & Louca 2007]. It is assumed that the time history of the loading overpressure $p(t)$ at a particular element can be represented by a typical wave profile with a single peak overpressure P and impulse I defined by

$$P = \max_{t_a \leq t < \infty} p(t) \,, \tag{1}$$

$$I = \int_{t_a}^{\infty} \max [p(t),\, 0] \ \mathrm{d}t \,, \tag{2}$$

where t is time and t_a is the arrival time of the shock wave. Many theoretical studies employ a single-degree-of-freedom model with the pressure time history approximated by the analytic expression

$$p(t) = P \exp \left[\frac{P \ (t_a - t)}{I} \right] \,, \quad t \geq t_a \,. \tag{3}$$

The behaviour of a structural element is modelled by an oscillating mass on a spring driven by the time-dependent force (3), and the maximum deflection of the mass from equilibrium can be explicitly obtained in terms of P and I [Baker et al. 1983]. Identifying the damage

level with the maximum deflection, it is straightforward to plot the corresponding iso-damage curve in the (P, I)-plane, which is called the P-I diagram. Typically, the P-I diagram looks like a shifted hyperbola approaching the pressure asymptote $P \to P_\infty$ as $I \to \infty$ (impulsive loading regime) and the impulse asymptote $I \to I_\infty$ as $P \to \infty$ (quasi-static loading regime).

However, the P-I diagram concept does not work well for the damage prediction of structural elements exposed to blast waves with multiple pulses, since the pressure time history cannot be described by just two parameters, P and I. In order to avoid the complicated problem of ambiguous extracting the peak overpressure and impulse from the pressure time history, a simple model based on the concept of accumulated damage is proposed. The accumulated damage is assumed to completely define the internal state of the structural element, and therefore its rate of change in time becomes a function of the damage itself and of the immediate environment modelled by the gas states at both sides of the thin structural element [Antanovskii 2008a, Antanovskii 2009]. This function has to be phenomenologically defined or experimentally measured after providing a rigorous definition of the accumulated damage, for example, by identifying it with the concentration of micro-fractures. The critical damage at which the element or a group of elements breaks has to be experimentally measured. A simple analytical expression for the rate of accumulated damage that involves a single empirical parameter called the cut-off overpressure is suggested. This approach allows one to estimate both the cut-off overpressure and the critical damage from the pressure and impulse asymptotes of the corresponding pressure-impulse diagram. Note that the accumulated damage is implicitly defined from the postulated expression for its rate.

A numerical scheme based on a Godunov-type solver [Godunov 1959] that employs the exact Riemann solver for flux calculation [Toro 1999], coupled with forward-time integration of the damage accumulation equation, is described. A pseudo-validation test and some illustrative numerical simulations in three dimensions are conducted, which demonstrate that the model is capable of capturing the essential physics and can be used in vulnerability studies, particularly when an accurate result is hard to predict due to a high level of uncertainties.

2   Mathematical model

The mathematical model consists of gas dynamics equations governing blast propagation inside and around a structure divided into compartments by internal rigid walls and frangible interfaces representing thin structural features like glass windows and bulkheads. The thin structural elements respond to blast loading at discrete times when the accumulated damage, governed by a certain damage accumulation equation, exceeds some threshold value. In this case the structural element is forced to fail thus dynamically changing the topology of the computational domain.

For the sake of simplicity, air and detonation products are modelled by a polytropic gas, and the effect of gravity is ignored. A more sophisticated model has to consider a multi-phase flow of a variable-composition mixture of gases. Bearing in mind the numerical finite-volume method to be employed, it is worth starting with the integral form of gas

dynamics equations.

Let t be time, ρ gas density, $\mathbf{v}$ velocity, p pressure, and e specific internal energy. The classical conservation laws of mass, momentum and energy for gas flow, written for arbitrary control volume ω with piecewise smooth boundary $\partial\omega$ oriented by inward normal unit vector $\mathbf{n}$, are as follows

$$\frac{\mathrm{d}}{\mathrm{d}t} \int_{\omega} \rho \, \mathrm{d}V = \int_{\partial\omega} \rho \, \mathbf{v} \cdot \mathbf{n} \, \mathrm{d}A \,, \tag{4}$$

$$\frac{\mathrm{d}}{\mathrm{d}t} \int_{\omega} \rho \, \mathbf{v} \, \mathrm{d}V = \int_{\partial\omega} \left(\rho \, \mathbf{v} \, \mathbf{v} \cdot \mathbf{n} + p \, \mathbf{n} \right) \mathrm{d}A \,, \tag{5}$$

$$\frac{\mathrm{d}}{\mathrm{d}t} \int_{\omega} \rho \left(e + \frac{1}{2} |\mathbf{v}|^2 \right) \mathrm{d}V = \int_{\partial\omega} \left[\rho \left(e + \frac{1}{2} |\mathbf{v}|^2 \right) + p \right] \mathbf{v} \cdot \mathbf{n} \, \mathrm{d}A \,. \tag{6}$$

Here $\mathrm{d}V$ and $\mathrm{d}A$ denote the volume and area elements, respectively.

The integral conservation laws imply the following Euler equations of gas dynamics written in the conservative form

$$\frac{\partial \rho}{\partial t} + \nabla \cdot (\rho \, \mathbf{v}) = 0 \,, \tag{7}$$

$$\frac{\partial (\rho \, \mathbf{v})}{\partial t} + \nabla \cdot (\rho \, \mathbf{v} \otimes \mathbf{v} + p \, G) = \mathbf{0} \,, \tag{8}$$

$$\frac{\partial}{\partial t} \left[\rho \left(e + \frac{1}{2} |\mathbf{v}|^2 \right) \right] + \nabla \cdot \left\{ \left[\rho \left(e + \frac{1}{2} |\mathbf{v}|^2 \right) + p \right] \mathbf{v} \right\} = 0 \,, \tag{9}$$

where ∇ denotes the gradient operator, $\otimes$ the tensor product, and G the metric tensor. The balance laws are completed with the constitutive equation for ideal polytropic gas [Courant & Friedrichs 1948]

$$p = (\gamma - 1) \, \rho \, e \tag{10}$$

where γ is the ratio of the specific heat at constant pressure, c_p, to the specific heat at constant volume, c_v.

Equations (7)–(10) constitute a self-contained model for gas flow. The model requires imposing initial and boundary conditions for gas density, internal energy and velocity.

The initial conditions for blast propagation are defined using the hot-gas balloon model for the products of detonation. For example, knowing the total mass and chemical energy of an explosive charge, it is straightforward to calculate the initial density and specific internal energy in an initial volume, usually a spherical balloon, occupied by the products of detonation. In most cases it suffices to set mass and energy densities uniform in the balloon and assume zero initial velocity. Finally, the specific heats ratio of the products of detonation is approximated by that of the air ($\gamma = 1.4$) to avoid the complex problem of multi-phase flow whose numerical solution exhibits spurious density profiles [Karni 1994]. It is conceivable that the far-field flow of gas is mainly influenced by the total mass and energy released from explosion.

Some attention should be paid to proper modelling of boundary conditions. The type of boundary conditions depends on the characteristics of the hyperbolic system of gas dynamics equations. In our situation only reflective and transmissive boundary conditions will be used, which are numerically modelled by introducing a layer of ghost cells just behind the boundary of the computational domain with an adjusted state of fictitious gas [Oran & Boris 1987]. Clearly, when a structural element fails, the boundary conditions change abruptly.

The interface state of a thin structural feature is completely described by accumulated damage δ considered a function of time and position point at the interface. If δ does not exceed some threshold value δ_*, the interface element is assumed rigid thus reflecting shock waves from both sides of the interface. However, when $\delta \geq \delta_*$, the interface element is forced to disappear with the effect of changing the reflecting boundary condition to natural condition between the adjacent control cells. Since, by definition, the state of a system determines its evolution, the rate of change of δ in time t depends on δ itself and the immediate state of environment. This results in the following ordinary differential equation

$$\frac{\mathrm{d}\delta}{\mathrm{d}t} = Q\left(\delta, p_+, p_-, \theta_+, \theta_-\right) \tag{11}$$

where Q is some non-negative function, and $p_\pm$ and $\theta_\pm$ denote the gas pressure and absolute temperature at both sides of the structural element, respectively. The function Q can be replaced with a differential operator to model crack propagation along the structure.

Assuming the pressure difference across the thin structure to be the main damage-causing mechanism, the following expression for damage accumulation is employed

$$Q = \max\left(|p_+ - p_-| - p_*, 0\right) \tag{12}$$

where p_* is some cut-off overpressure depending on the material and dimensions of the structure. It is clear that, if the overpressure $|p_+ - p_-|$ is less than p_*, the damage rate (12) vanishes and hence no increase of the accumulated damage is observed.

To the first approximation the parameters p_* and δ_* can be estimated from the pressure-impulse diagram as $p_* = P_\infty$ and $\delta_* = I_\infty$. Indeed, δ and δ_* have the dimension of impulse defined by the time integral of pressure according to Equation (2). It is conceivable that, if the overpressure $|p_+ - p_-|$ does not exceed the value of the pressure asymptote P_∞, there is no structural failure irrespective of the impulse. Therefore, the value of the pressure asymptote has the meaning of the cut-off overpressure p_*. Similarly, if the impulse is less than the value of the impulse asymptote, the structural element does not fail irrespective of the peak overpressure. For high pressure compared to p_*, the impulse is close to the accumulated damage δ as can be seen from Equations (11) and (12), and therefore the impulse asymptote can be identified with δ_*.

It is worthwhile noting that Equation (11), with given expression for the right-hand side (12), implicitly defines the accumulated damage δ by assuming that initially $\delta = 0$.

3   Numerical algorithm

The employed numerical model involves simultaneous solution of the Euler equations (7)–(10) and damage accumulation equation (11) with the right-hand side (12). The gas dynamics equations are solved by an explicit Godunov-type conservative scheme [Godunov 1959] based on the finite-volume method coupled with the exact Riemann solver for flux evaluation between the adjacent control cells [Toro 1999]. As a by-product of the Riemann solver, the gas state at each facet between two control cells in contact, including the boundary and ghost cells, is calculated, which is used to evaluate the damage rate from Equation (12). The accumulated damage δ is calculated at each boundary facet representing a structural feature using the explicit forward-time Euler scheme. When the maximum value of δ over a group of facets representing the structural feature exceeds δ_*, all the facets of the group fail thus changing the internal boundary conditions.

In order to uniformly handle different types of mesh, either structured or unstructured, the control cells and facets separating them are represented by a directed graph [Antanovskii 2008b]. The vertices and arcs of the directed graph correspond to the control cells and facets, respectively. The graph is directed because each facet must be oriented. This identification is possible because every facet has exactly two adjacent cells, since every cell attached to the boundary has a corresponding ghost cell. The directed graph changes dynamically whenever any facet fails.

Let us introduce the volumetric density of momentum, $\mathbf{u} = \rho\,\mathbf{v}$, and the volumetric density of total energy, $\varepsilon = \rho\left(e + \frac{1}{2}\,|\mathbf{v}|^2\right)$. In terms of these conserved variables the conservation laws (4)–(6) take the succinct form

$$\frac{\mathrm{d}}{\mathrm{d}t}\int_{\omega} [\rho,\,\mathbf{u},\,\varepsilon]\ \mathrm{d}V = \int_{\partial\omega}\left[\mathbf{u}\cdot\mathbf{n},\,\frac{1}{\rho}\,\mathbf{u}\,\mathbf{u}\cdot\mathbf{n} + p\,\mathbf{n},\,\frac{\varepsilon + p}{\rho}\,\mathbf{u}\cdot\mathbf{n}\right]\mathrm{d}A \tag{13}$$

where

$$p = (\gamma - 1)\left(\varepsilon - \frac{|\mathbf{u}|^2}{2\rho}\right) \tag{14}$$

according to the equation of state (10). Let $\{\omega_i\}$ $(i = 1,\ldots,N_c)$ constitute tessellation of the computational domain $\mathcal{D}$ where N_c is the total number of control cells. The state of the gas dynamics flow is approximated by the cell average values

$$S_i = \frac{1}{V_i}\int_{\omega_i} [\rho,\,\mathbf{u},\,\varepsilon]\ \mathrm{d}V \tag{15}$$

and the fluxes by the surface integrals

$$R_i = \frac{1}{V_i}\int_{\partial\omega_i}\left[\mathbf{u}\cdot\mathbf{n},\,\frac{1}{\rho}\,\mathbf{u}\,\mathbf{u}\cdot\mathbf{n} + p\,\mathbf{n},\,\frac{\varepsilon + p}{\rho}\,\mathbf{u}\cdot\mathbf{n}\right]\mathrm{d}A \tag{16}$$

where

$$V_i = \int_{\omega_i}\mathrm{d}V \tag{17}$$

is the cell volume. According to the conservation laws (13) and the equation of state (14), the following system of ordinary differential equations results

$$\frac{\mathrm{d}S_i}{\mathrm{d}t} = R_i \,. \tag{18}$$

In order to complete this system of dynamic equations one needs to express the rates R_i in terms of the states S_i. This is done by employing the Riemann solver which allows one to explicitly determine the fluxes between two cells in contact, provided that the gas states in the cells are approximated by constant values and the cells are separated by a planar patch. In this case the cell average values S_i are approximated by the first order quadrature formulae

$$S_i = [\rho_i, \, \mathbf{u}_i, \, \varepsilon_i] \,. \tag{19}$$

Let us assume that the collection $\{\omega_i\}$ $(i = 1, \ldots, N_c)$ is composed of polyhedra, potentially of different type, and let $\{\varphi_k\}$ $(k = 1, \ldots, N_f)$ be the collection of all distinct facets of the polyhedra. The ghost cells are already included in the collection of polyhedra. The state of the ghost cell must be specified to model the appropriate boundary conditions [Oran & Boris 1987]. Denote the area of facet φ_k by A_k, select a unit normal vector $\mathbf{n}_k$, and introduce a N_f-by-2 facet-to-cell connectivity matrix α with entries defined as follows. If facet φ_k belongs to the intersection $\partial\omega_{i_1} \cap \partial\omega_{i_2}$ and $\mathbf{n}_k$ points from ω_{i_1} to ω_{i_2}, then set $\alpha(k, 1) = i_1$ and $\alpha(k, 2) = i_2$. Mathematically, the cell connectivity matrix α defines a directed graph $(\mathcal{V}, \mathcal{E})$ where vertices $\mathcal{V}$ are cells (including the ghost cells) and edges $\mathcal{E}$ are facets.

The numerical algorithm is straightforward. First update the states of the ghost cells according to the imposed boundary conditions. For example, for an ideally reflective wall or symmetry plane, set the ghost cell state equal to that of the neighbouring boundary cell except for the normal component of momentum which must have the opposite sign. For transmissive boundary condition, set the ghost cell state identical to the boundary cell state. Then, for given S_i at some instant t, calculate the cell values of velocity $\mathbf{v}_i = \mathbf{u}_i/\rho_i$ and pressure p_i from Formula (14). Zero out the array of rates R_i. For each facet φ_k solve the Riemann problem [Toro 1999] using the given gas states in cells ω_{i_1} and ω_{i_2} where $i_1 = \alpha(k, 1)$ and $i_2 = \alpha(k, 2)$. Knowing the gas state at the facet calculate the fluxes of mass, momentum and energy along the unit normal vector $\mathbf{n}_k$, multiply by the facet area A_k, and add to the rate R_{i_2} but subtract from the rate R_{i_1} according to the choice of the normal $\mathbf{n}_k$. Finally, divide the calculated rates R_i by volumes V_i. This procedure defines the cell rates $\{R_i\}$ as a function of the cell states $\{S_i\}$.

The accumulated damage is approximated by a constant value δ_k defined at each facet φ_k representing the thin structural feature. Equations (11) and (12) naturally transform to the system of equations

$$\frac{\mathrm{d}\delta_k}{\mathrm{d}t} = \max\left(\left|p_k^+ - p_k^-\right| - p_*, 0\right) \tag{20}$$

where $p_k^{\pm}$ are the interface pressures at both sides of the facet obtained from the solution of the Riemann problems as a by-product.

As a result of this procedure one ends up with a non-linear system of ordinary differential equations that can be solved by the explicit Euler scheme. The size of the time

step is selected according to the Courant–Friedrichs–Lewy (CFL) condition which requires estimation of velocity and sound speed at the cell interfaces. Physically, this condition limits the time step to the value small enough not to allow Riemann waves to propagate more than half size of a control cell.

Two different approaches for mesh representation are considered. In the first approach the mesh is represented by a global directed graph whose vertices, edges and the connectivity matrix change dynamically whenever any facet fails. This requires to implement a quite complicated logic as the control cells of new compartments have to be dynamically added that changes the numerical model size and may cause memory problems. In the second approach the mesh is represented by a collection of directed graphs, one directed graph per compartment. The allocated memory does not change during program execution as different directed graphs exchange information through their own ghost cells. The calculations are performed only for those compartments which are affected by the blast. Though the number of cells is slightly increased, the second approach is more flexible as the coding logic is considerably simplified, and at the same time it allows one to implement a parallel multi-threaded or multi-CPU code, because after updating the states of the ghost cells of the directed graphs the Riemann solvers can be executed on different processors independently.

The described numerical algorithm is implemented in DBlast, a DSTO software for simulation of blast loads on structures. A MATLAB® graphical interface for post-processing is developed.

4   Simulation results

All the simulations are conducted for air ($c_v = 716.46\,\text{J/kg/K}$, $c_p = 1003.51\,\text{J/kg/K}$) initially kept at atmospheric pressure $p = 101.325\,\text{kPa}$ and absolute temperature $\theta = 288\,\text{K}$ ($15°\,\text{C}$). It is assumed that an explosive charge of trinitrotoluene (TNT) is initiated from its centre, and all the chemical reactions are completed when the spherical detonation wave reaches the charge boundary. Therefore, the initial density of the products of detonation is equal to the density of the condensed TNT explosive, $\rho = 1.6 \times 10^3\,\text{kg/m}^3$, and the initial internal energy is the chemical energy released, $e = 4.52 \times 10^6\,\text{J/kg}$.

4.1   Model validation

The pure gas dynamics solver of DBlast has been successfully validated against several benchmark solutions, such as Sod's shock tube problem [Sod 1978], along the lines of the gas dynamics solver previously developed in MATLAB® [Antanovskii 2008b]. In addition to this, the validation of DBlast against Air3D developed by Rose [2006] and ConWep (Conventional Weapons Effects Calculator) has been conducted. A spherically symmetric blast from a spherical 100 kg charge of TNT has been simulated in three-dimensions by DBlast and Air3D using exactly the same mesh of cubic cells. The computational domain is a cube of edge length 5 m, and the cell size is 25 mm. The charge is centred at one corner of the cube, the origin $(0, 0, 0)$ of the Cartesian coordinate system (x, y, z) aligned with three cube edges, and the three-dimensional solution has three planes of symmetry $x = 0$, $y = 0$,

and $z = 0$, where reflective boundary conditions are imposed. Transmissive boundary conditions are imposed at the opposite faces of the cube. The pressure gauge points are specified at the space diagonal of the cube at 4 m and 5 m stand-off distances. The pressure time history shown in Figure 1 demonstrates farely good agreement with Air3D and ConWep. It is worthwhile noting that Air3D uses a different numerical algorithm, whereas ConWep is based on real empirical data.

A pseudo-validation test described in Example 4 (Testing Glazing in a Cubicle Structure) of Air3D users' guide [Rose 2006] has been simulated by DBlast. The laminated glass pane of dimensions 1.25 m by 1.55 m by 7.5 mm has been selected as the glazing element. As is indicated by Johnson [1999], the 4.536 kg charge of TNT at 8 m stand-off, detonated 1 m above the ground, is sufficient to cause breakage of the laminated glass window in a cubicle structure with frontal dimensions 2.15 m by 2.15 m and length 3 m, whereas 3 kg, at the same stand-off, is not. The simulation results obtained with the use of Air3D confirm this assertion.

Table 1: *P-I data for a laminated glass pane of dimensions* 1.25 m *by* 1.55 m *by* 7.5 mm.

P (kPa)	2,000	100	70	46	30	23	20	18	17.5	16.7	16
I (kPa × ms)	175	180	185	200	250	300	400	500	700	1,000	10,000

The corresponding P-I diagram for the glazing element (taken from [Rose 2006]) is tabulated in Table 1 and plotted in Figure 2. It is clear that the values for the asymptotes of the P-I diagram are as follows

$$p_* = 16\,\text{kPa}\,, \quad \delta_* = 175\,\text{kPa} \times \text{ms}\,. \tag{21}$$

The geometry of the computational domain is shown in Figure 3, where the solution is assumed to have two planes of symmetry, $x = 0$ and $y = 0$. The obtained results simulated by DBlast have predicted the same effect as Air3D, and even the time of window breakage is virtually identical. The pressure time history at the centre of the glass window and the accumulated damage normalised by the critical damage δ_* are depicted in Figure 4 for 3 kg charge and Figure 5 for 4.536 kg charge.

4.2   Blast propagation inside a building

The geometry for the simulated three-dimensional structure is shown in Figure 6. The two-room building contains seven windows, one of which is internal, of the same dimensions as indicated in Table 1, so the cut-off overpressure and critical damage are given by Formulae (21). The walls are 0.5 m thick, and any doors, if present, are shut. A spherical 15 kg charge of TNT explosive is placed at position $x = 4\,\text{m}$, $y = 1\,\text{m}$, $z = 0.5\,\text{m}$ of the depicted Cartesian coordinate system. In Figure 6 the charge can be seen through two windows as a red sphere. The computational domain of this example consists of $7,504,530$ cubical cells (excluding ghost cells) and $22,762,238$ square faces. It suffices to choose the CFL number equal to 0.5 to achieve numerical stability that resulted in $3,016$ cycles to complete the simulations for the final 20 ms physical time.

The pressure time history at two gauge points located at the middle of each room (floor level) is shown in Figure 7. Here Room 1 refers to the larger room where the

charge is positioned, whereas Room 2 is the smaller one. The pressure contours in the vertical ($y = 3\,\mathrm{m}$) and horizontal ($z = 1\,\mathrm{m}$) cross-sections are displayed in Figures 8–15 for increasing instances of time. It is seen that the windows fail in turn, thus allowing the blast to propagate into the adjacent room (Room 2) and outside of the building.

5   Discussion

The described model is significantly simpler as compared to more sophisticated fluid-structure interaction models. Nevertheless, it is capable of capturing the effect of progressive failure of thin structural elements, like windows and light bulkheads, followed by blast transfer into adjacent compartments. In many circumstances there is little information about the details of a compartmented structure and the charge characteristics, and therefore only rough estimates for the level of damage of vulnerable components hidden inside the structure is required. In this case it is worthwhile considering as simple model as possible to avoid unnecessary handling of uncertain details.

The pressure-impulse diagrams (iso-damage curves) are used for the prediction of damage of other materials not necessarily glasses, and for the evaluation of the response of various components to blast loading. However, the simplified assumption that the structural feature completely disappears when the accumulated damage reaches some threshold is applicable to sufficiently thin elements composed of a low-density material.

Note that the proposed model does not take into account the dynamics of debris and the associated exchange of momentum and energy between the blast and fragments. This shortcoming can be overcome by considering a more complex model for the structural element. For example, it can be modelled by a layer of three-dimensional rigid elements, not necessarily of zero thickness, until it breaks. The break point has to be determined by a similar criterion for accumulated damage. After breaking, the material of the rigid elements is replaced with a fictitious gas of high density and of different equation of state (i.e. different specific heats ratio). The effect of debris can be modelled by the fictitious gas, and the coupled dynamics of blast and fragments will be governed by a multi-phase flow model. The enhanced model does not track each individual fragment as the fictitious gas represents only the average mass of fragments. The development of the described multi-phase model for blast and fragment synergy will be the subject of a separate study.

The concept of accumulated damage, widely used in fatigue theory, can be equally applied to vulnerable components placed inside a structure. The component's accumulated damage normalised by its critical damage can be regarded as the probability of failure of the component. This approach replaces the notion of failure probability, which is very hard to measure and thus difficult to validate the corresponding model, with a conceptually simpler notion of accumulated damage governed by a dynamic equation.

References

Antanovskii, L. K. (2008*a*) Blast propagation in domains of changing topology, *in XXII International Congress of Theoretical and Applied Mechanics*, Adelaide, Australia.

Antanovskii, L. K. (2008*b*) *Solving multi-dimensional problems of gas dynamics using MATLAB®*, Technical Report DSTO–TR–2139, DSTO, Edinburgh, Australia.

Antanovskii, L. K. (2009) Blast propagation in compartmented structures with progressively failing thin bulkheads, *in 8th International Conference on Shock & Impact Loads on Structures*, Adelaide, Australia, pp. 153–160.

Baker, W. E. (1973) *Explosions in Air*, University of Texas Press, Austin.

Baker, W. E., Cox, P. A., Westine, P. S., Kulesz, J. J. & Strehlow, R. A. (1983) *Explosion Hazards and Evaluation*, Vol. 5 of *Fundamental Studies in Engineering*, Elsevier, Amsterdam.

Bangash, M. Y. H. (1993) *Impact and Explosion: Analysis and Design*, Blackwell Scientific Publications, Oxford.

Cluttera, J. K., Mathis, J. T. & Stahl, M. W. (2007) Modeling environmental effects in the simulation of explosion events, *Intern. J. Impact Engng* **34**(5), 973–989.

Courant, R. & Friedrichs, K. O. (1948) *Supersonic Flow and Shock Waves*, Interscience, London.

Dowell, E. H. & Hall, K. C. (2001) Modelling of fluid–structure interaction, *Ann. Rev. Fluid Mech.* **33**, 445–490.

Fallah, A. S. & Louca, L. A. (2007) Pressure-impulse diagrams for elastic-plastic-hardening and softening single-degree-of-freedom models subjected to blast loading, *Intern. J. Impact Engng* **34**(4), 823–842.

Gelfand, B. E. & Silnikov, M. V. (2004) *Explosions and Blast Control*, Asterion, St Petersburg.

Godunov, S. K. (1959) A difference scheme for numerical computation of discontinuous solutions of hydrodynamic equations, *Math. Sbornik* **47**(3), 271–306. In Russian.

Gong, M. & Andreopoulos, Y. (2009) Coupled fluid-structure solver: The case of shock wave impact on monolithic and composite material plates, *J. Comp. Phys.* **228**(12), 4400–4434.

Johnson, N. F. (1999) European blast resistant glazing standards: The shock tube and range tests compared, *in 9th International Symposium on the Interaction of the Effects of Munitions with Structures*, Strausberg, Germany.

Jones, N. & Brebbia, C. A., eds (2006) *Structures under Shock and Impact IX*, WIT Press, Southampton, UK.

Karni, S. (1994) Multicomponent flow calculations by a consistent primitive algorithm, *J. Comput. Phys.* **112**(1), 31–43.

Lloyd, R. M. (1998) *Conventional Warhead Systems: Physics and Engineering Design*, Vol. 179 of *Progress in Astronautics and Aeronautics*, American Institute of Aeronautics & Astronautics, Reston, VA.

Oran, E. S. & Boris, J. P. (1987) *Numerical Simulation of Reactive Flow*, Elsevier, New York.

Remennikov, A. M. & Rose, T. A. (2005) Modelling blast loads on buildings in complex city geometries, *Computers & Structures* **83**(27), 2197–2205.

Remennikov, A. M. & Rose, T. A. (2007) Influence of the principal geometrical parameters of straight city streets on positive and negative phase blast wave impulses, *Intern. J. Impact Engng* **34**(12), 1907–1923.

Rose, T. A. (2006) A computational tool for airblast calculations. Air3d version 9 users' guide.

Rose, T. A. & Smith, P. D. (2002) Influence of the principal geometrical parameters of straight city streets on positive and negative phase blast wave impulses, *Intern. J. Impact Engng* **27**(4), 359–376.

Smith, P. D. & Rose, T. A. (2002) Blast loading and building robustness, *Prog. Struct. Engng Mater.* **4**(2), 213–223.

Smith, P. D. & Rose, T. A. (2006) Blast wave propagation in city streets—an overview, *Prog. Struct. Engng Mater.* **8**(1), 16–28.

Sod, G. A. (1978) A survey of several finite difference methods for systems of nonlinear hyperbolic conservation laws, *J. Comp. Phys.* **27**(1), 1–31.

Toro, E. F. (1999) *Riemann Solvers and Numerical Methods for Fluid Dynamics: A Practical Introduction*, 2nd edn, Springer, Berlin.

Zhou, X., Hao, H. & Deeks, A. J. (2005) Numerical simulation of blast wave propagation in a building structure, *in Recent Advances in Counter–Terrorism Technology and Infrastructure Protection: Proceedings of the 2005 Science, Engineering and Technology Summit*, Australian Homeland Security Research Centre, ACT, Australia.
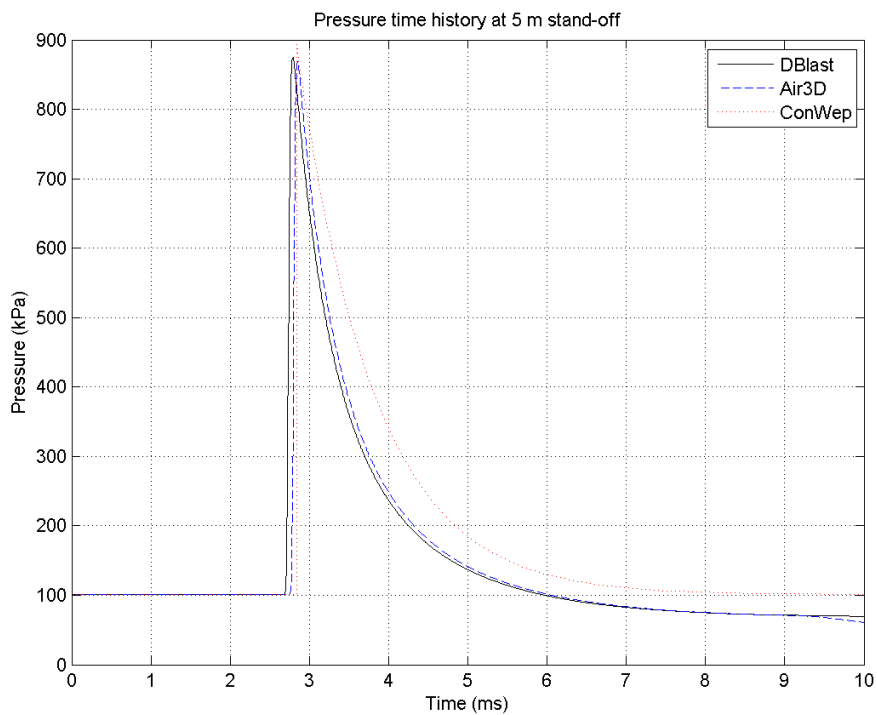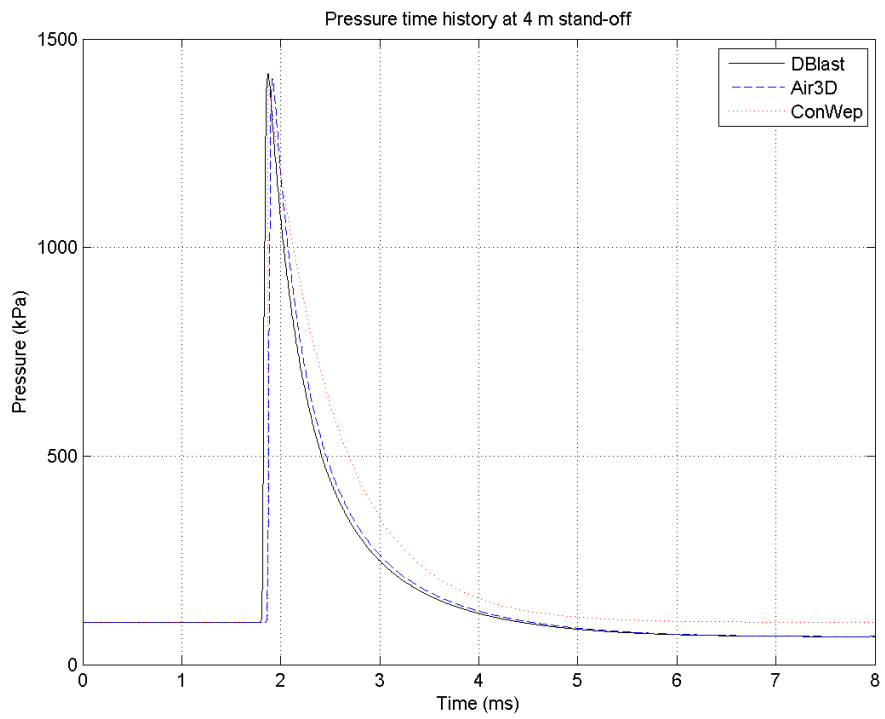
**Figure 1:** *Validation of pure gas dynamics solver of DBlast against Air3D and ConWep.*
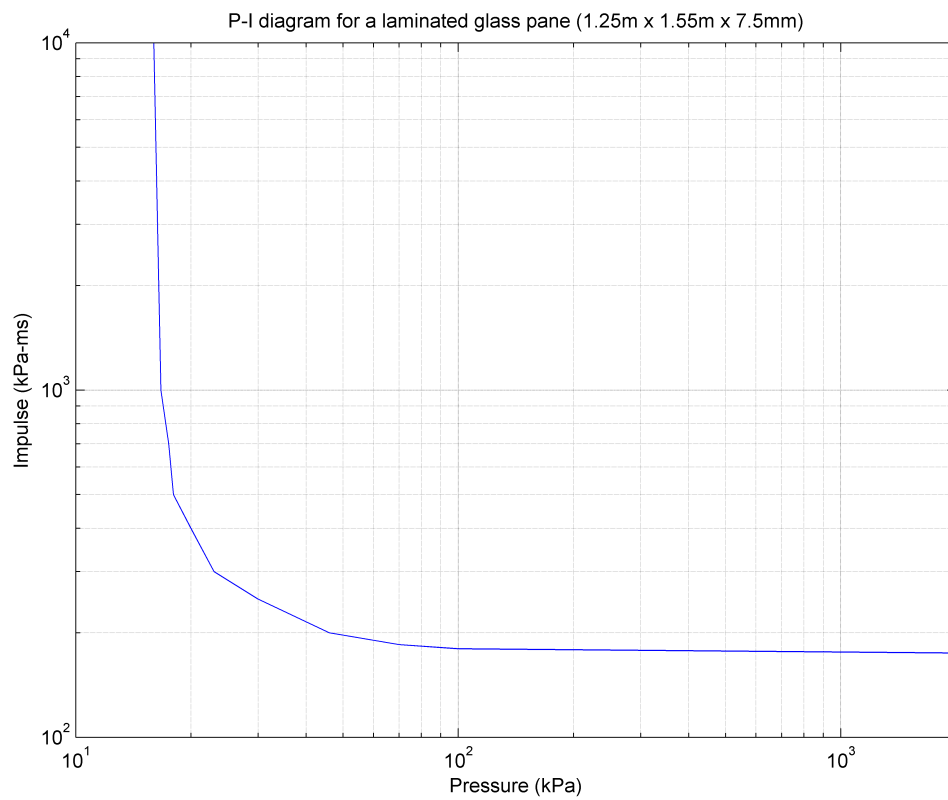
*Figure 2: P-I diagram for a laminated glass pane as in Table 1.*
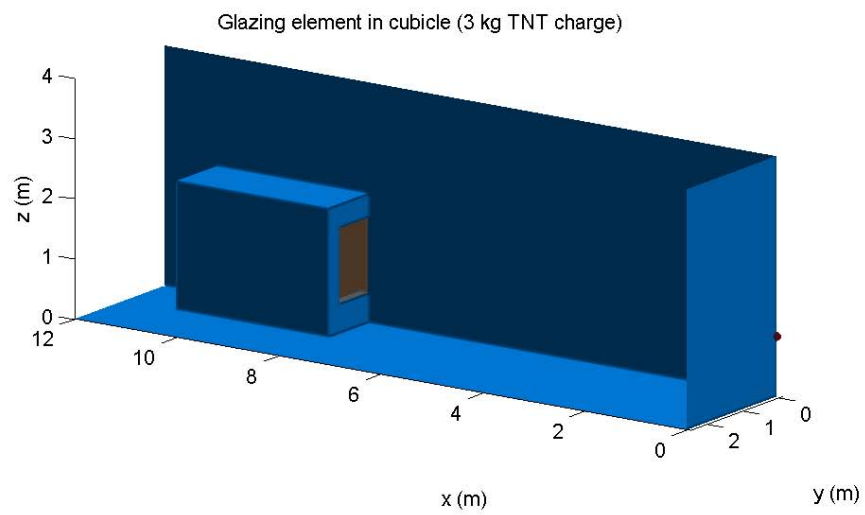
*Figure 3: Computational domain for testing a window element in a cubicle.*
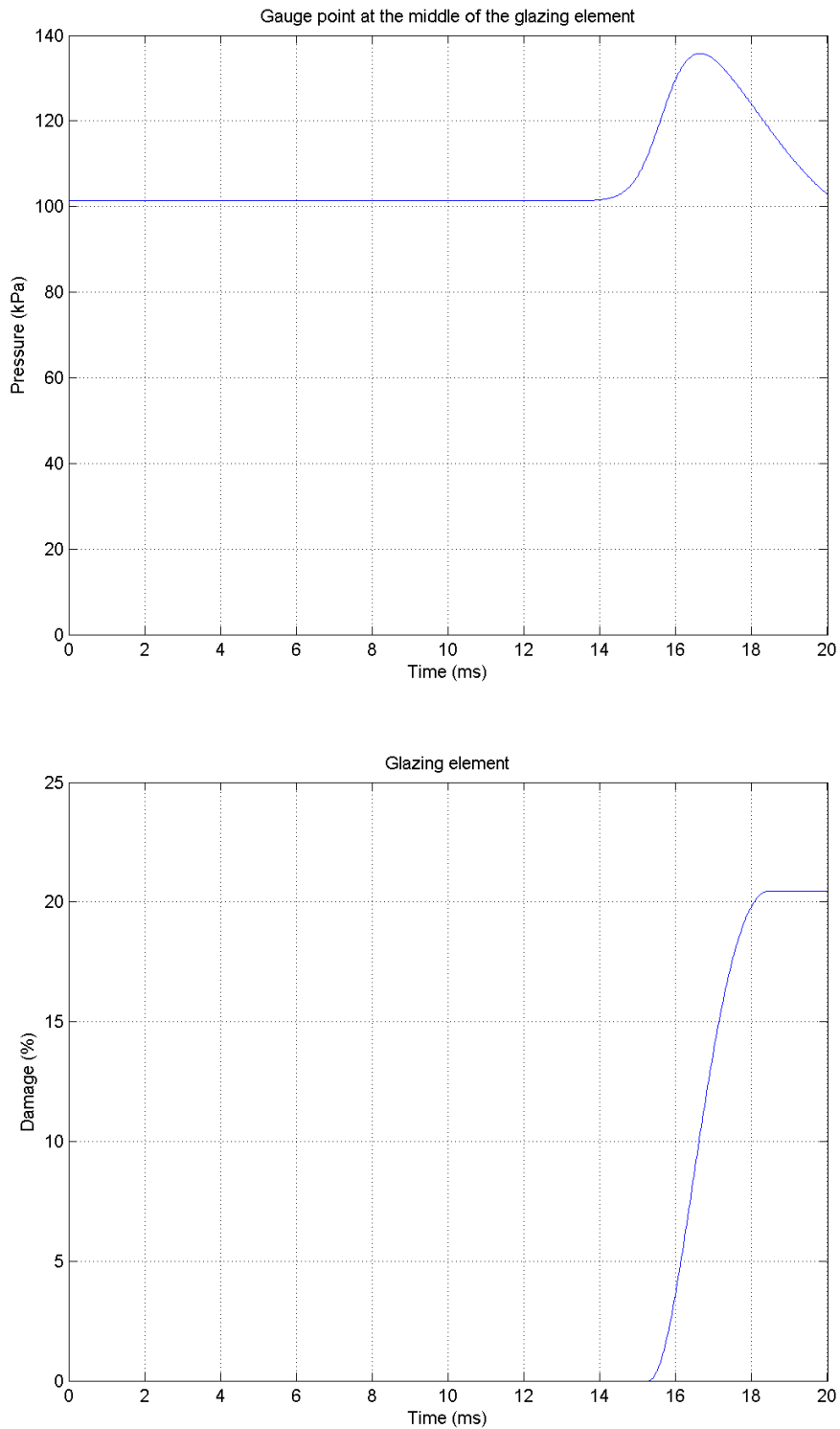
Figure 4: *Pressure time history at the centre of the window element in a cubicle and normalised damage for* 3 kg *TNT charge.*
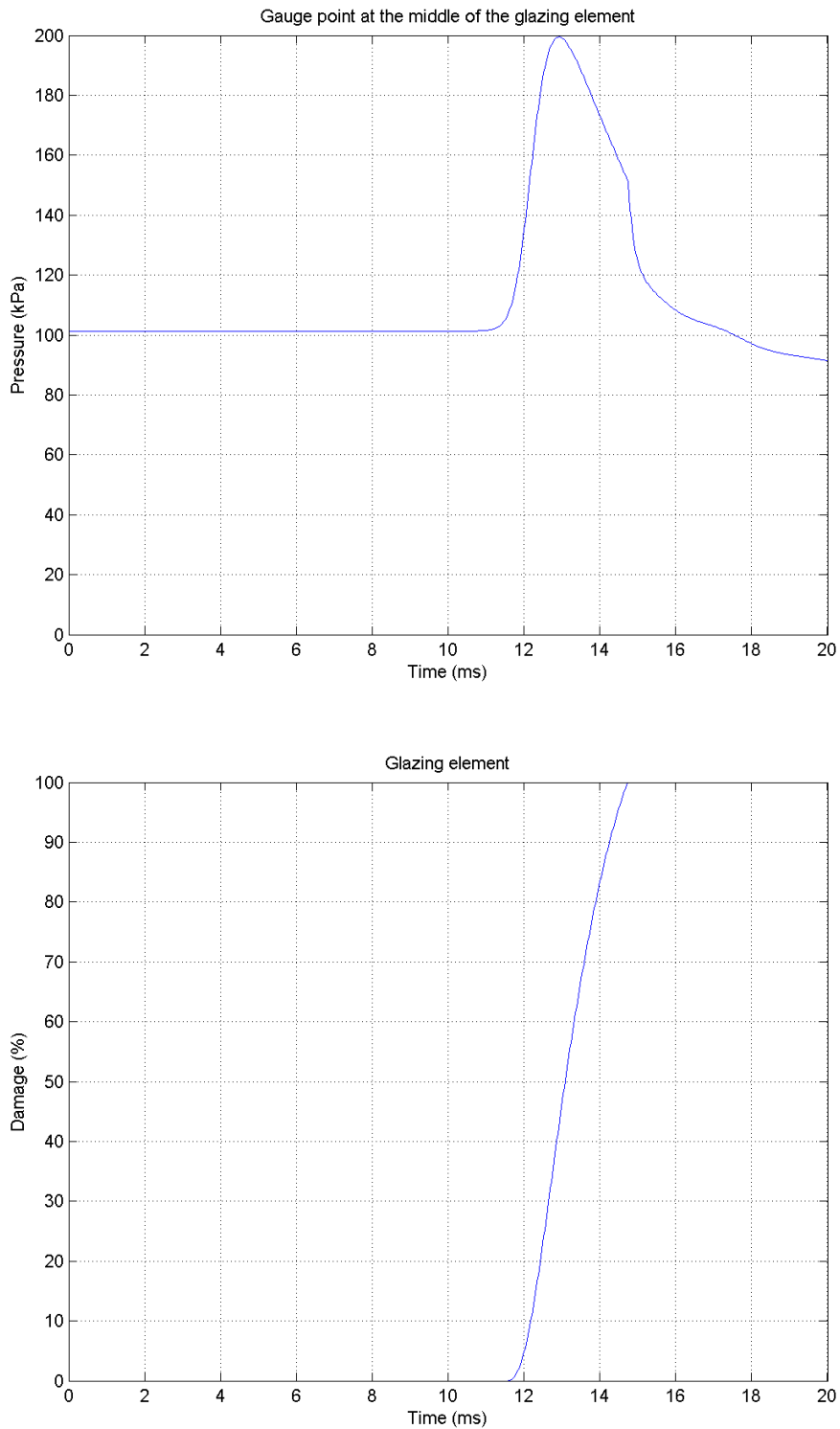
**Figure 5:** *Pressure time history at the centre of the window element in a cubicle and normalised damage for 4.536 kg TNT charge.*

Blast propagation inside a building
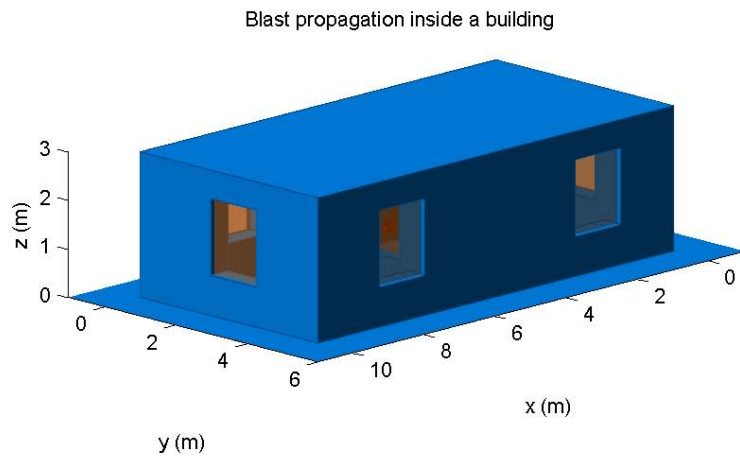
Figure 6: *Building geometry.*
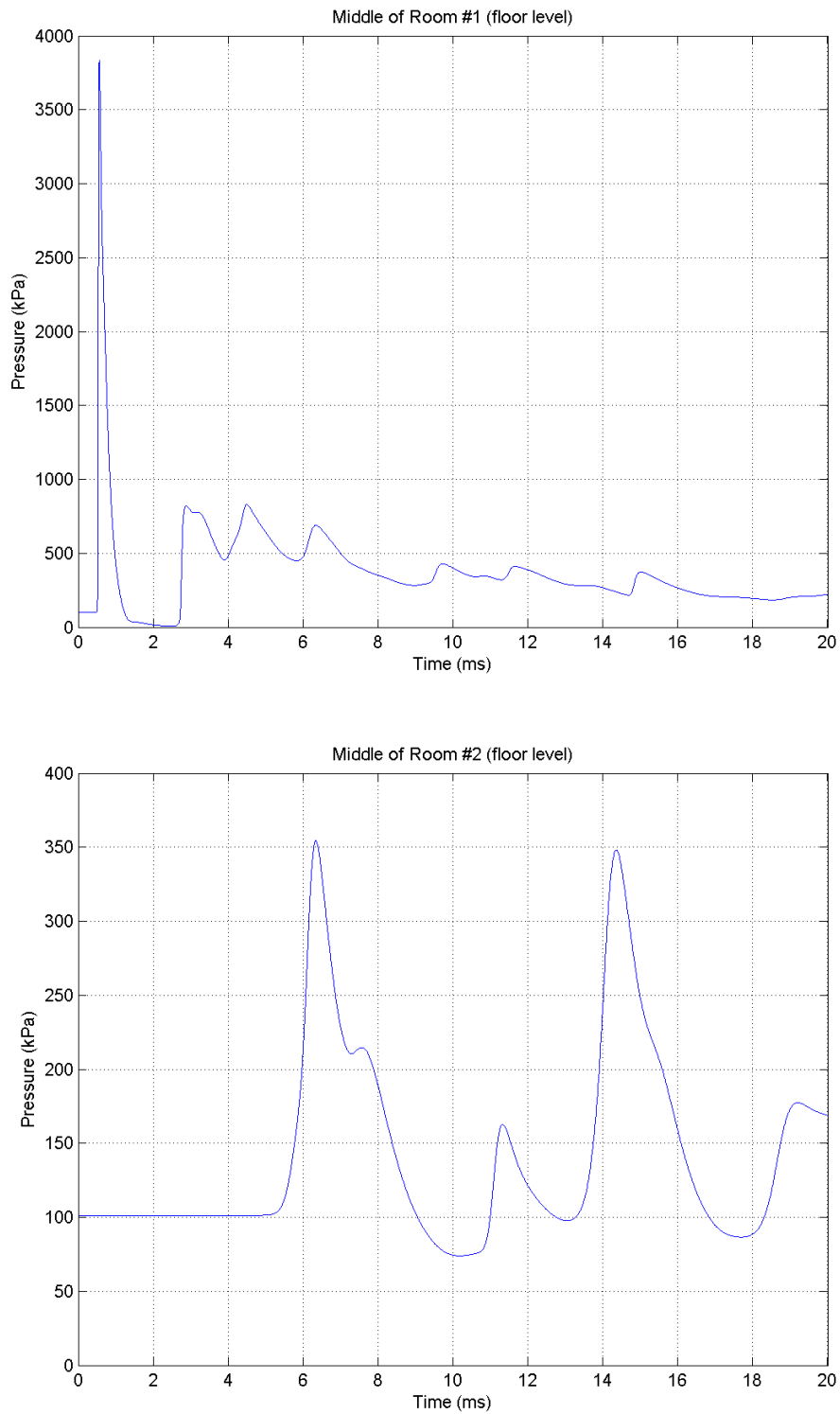
Figure 7: *Pressure time history at the middle of Room 1 and Room 2 (floor level).*
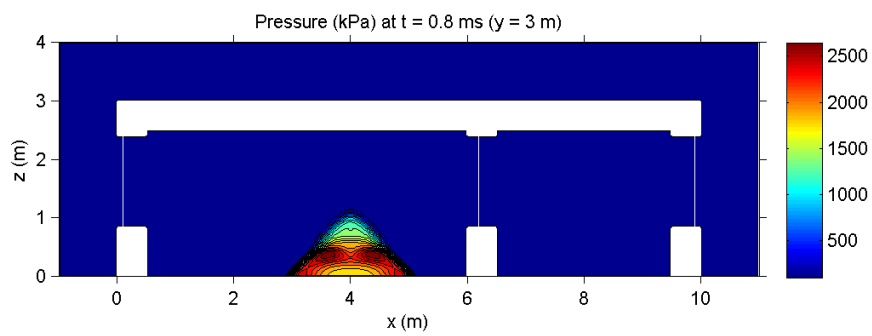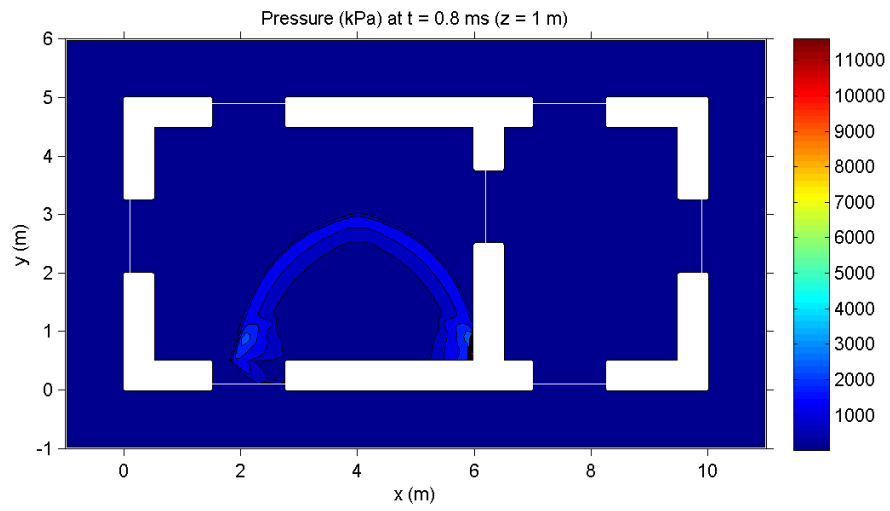
Figure 8: *Pressure contours in the horizontal and vertical cross-sections at $t = 0.8$ ms.*
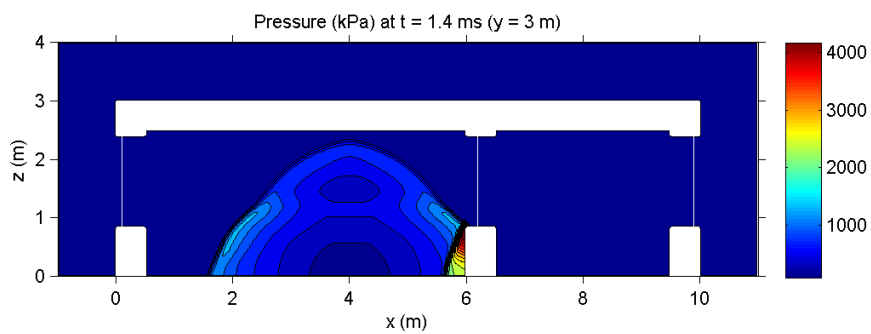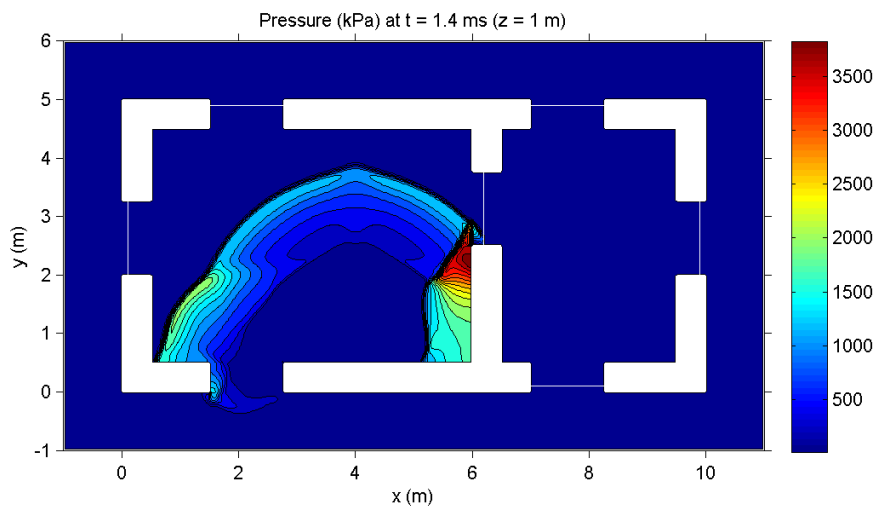
**Figure 9:** *Pressure contours in the horizontal and vertical cross-sections at* $t = 1.4\,\text{ms}$.
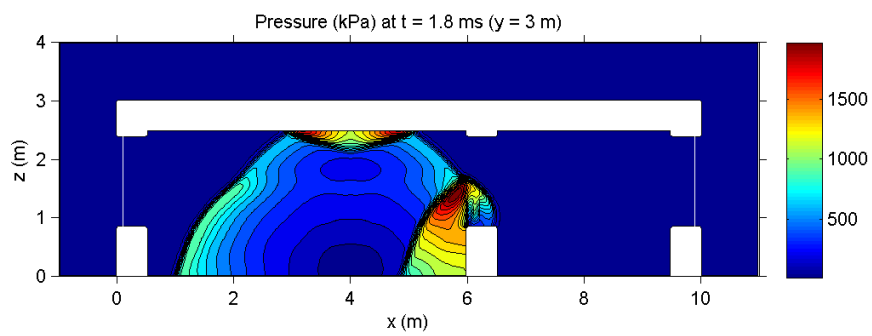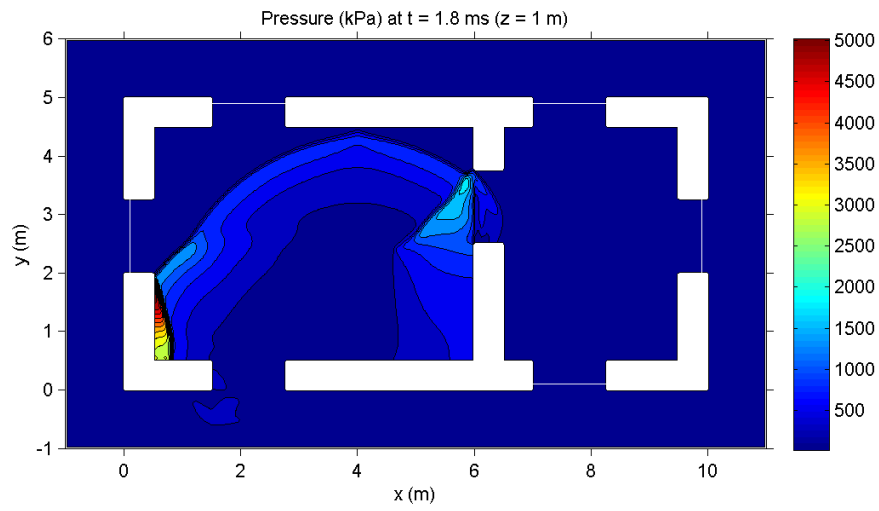
Figure 10: *Pressure contours in the horizontal and vertical cross-sections at* $t = 1.8$ ms.
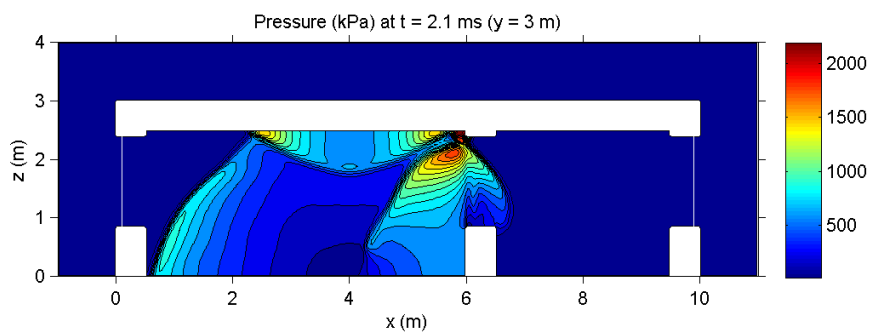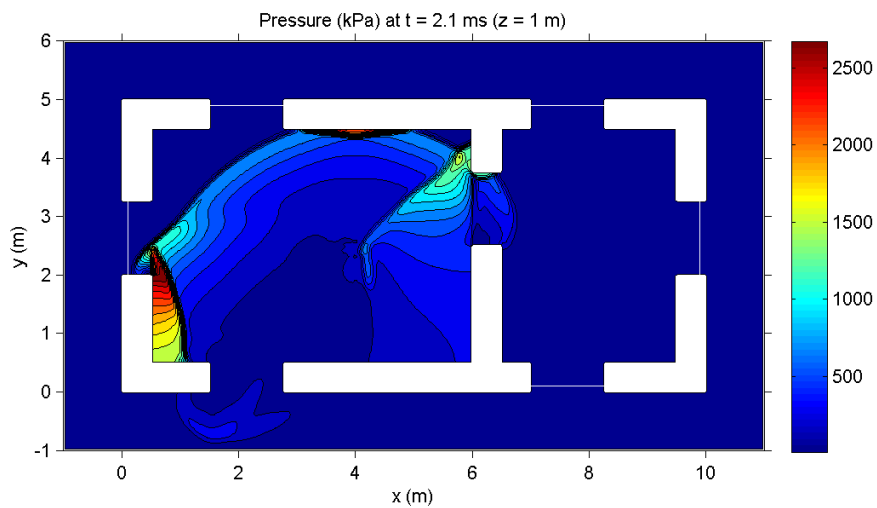
Figure 11: *Pressure contours in the horizontal and vertical cross-sections at $t = 2.1$ ms.*
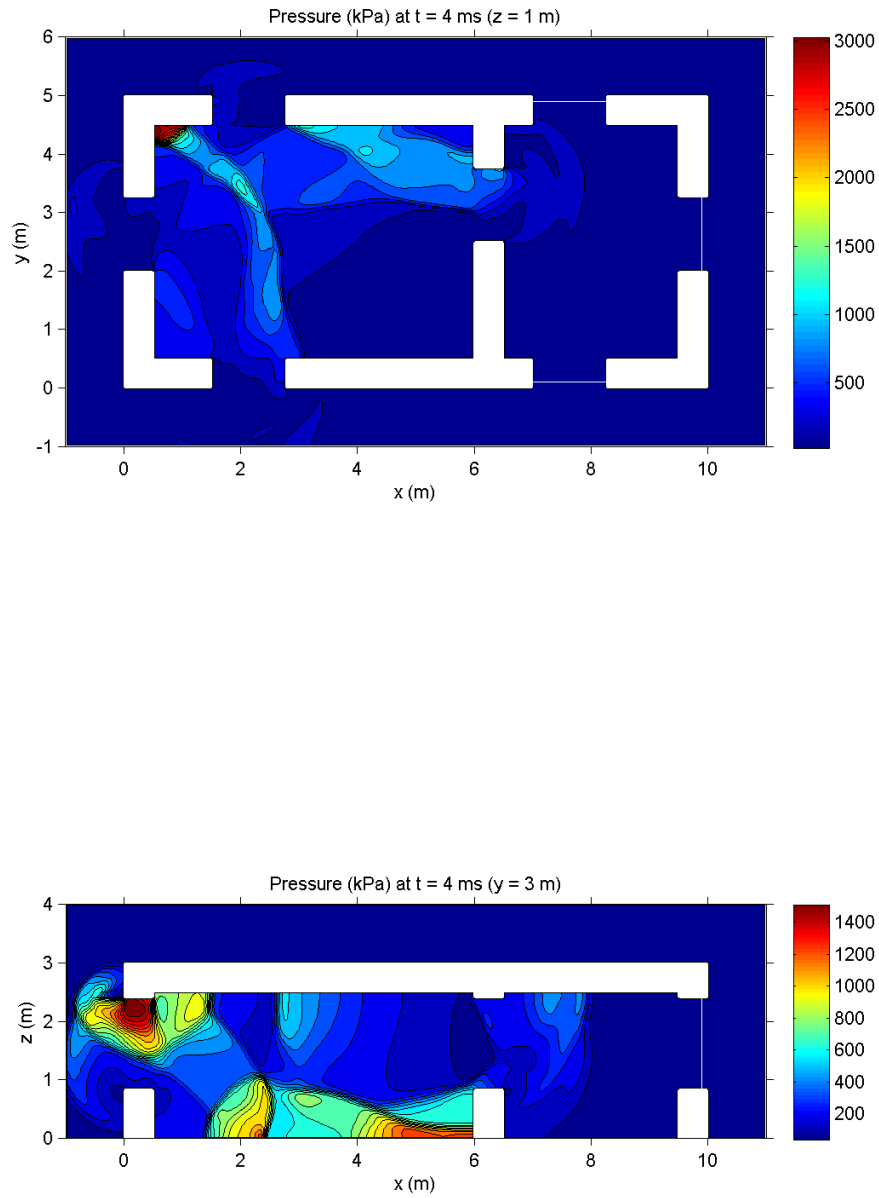
Figure 12: *Pressure contours in the horizontal and vertical cross-sections at* $t = 4$ ms.
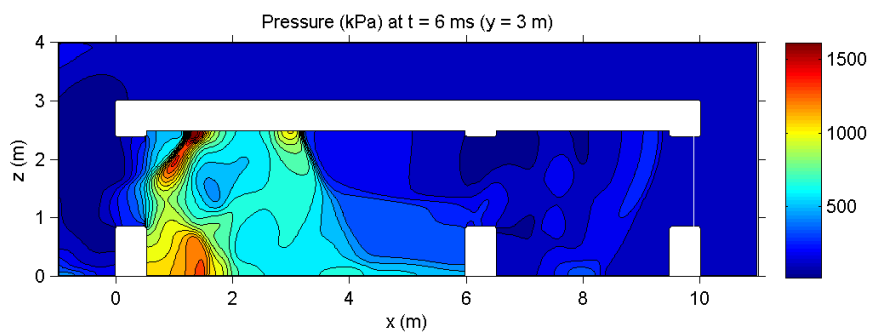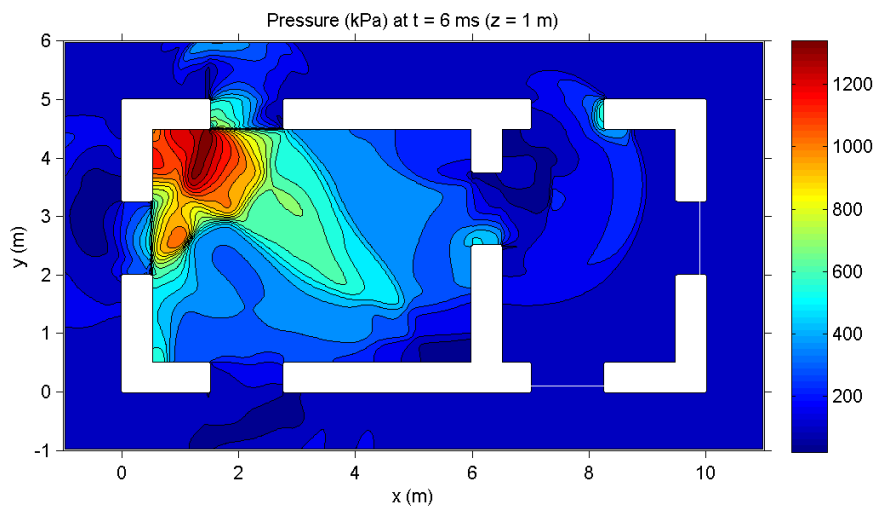
Figure 13: *Pressure contours in the horizontal and vertical cross-sections at* $t = 6\,\mathrm{ms}$.
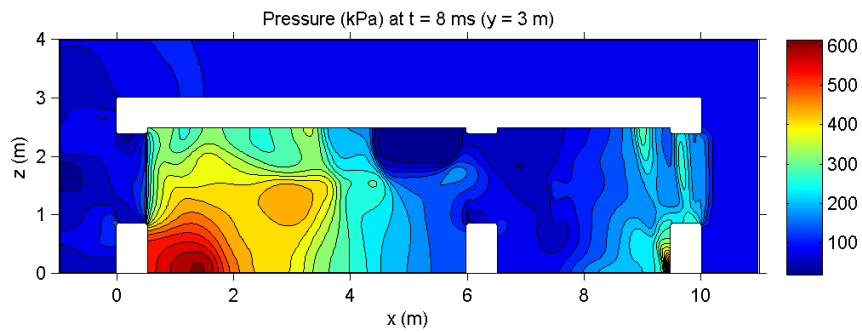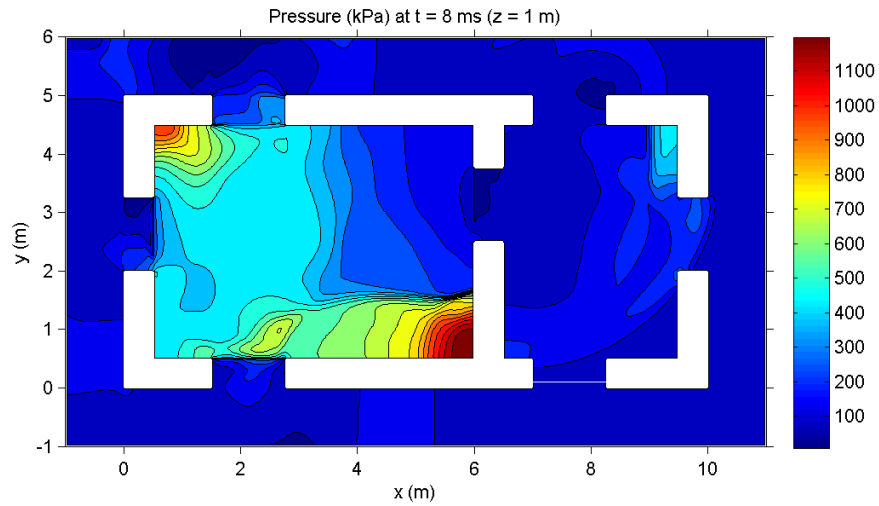
Figure 14: *Pressure contours in the horizontal and vertical cross-sections at* $t = 8$ ms.
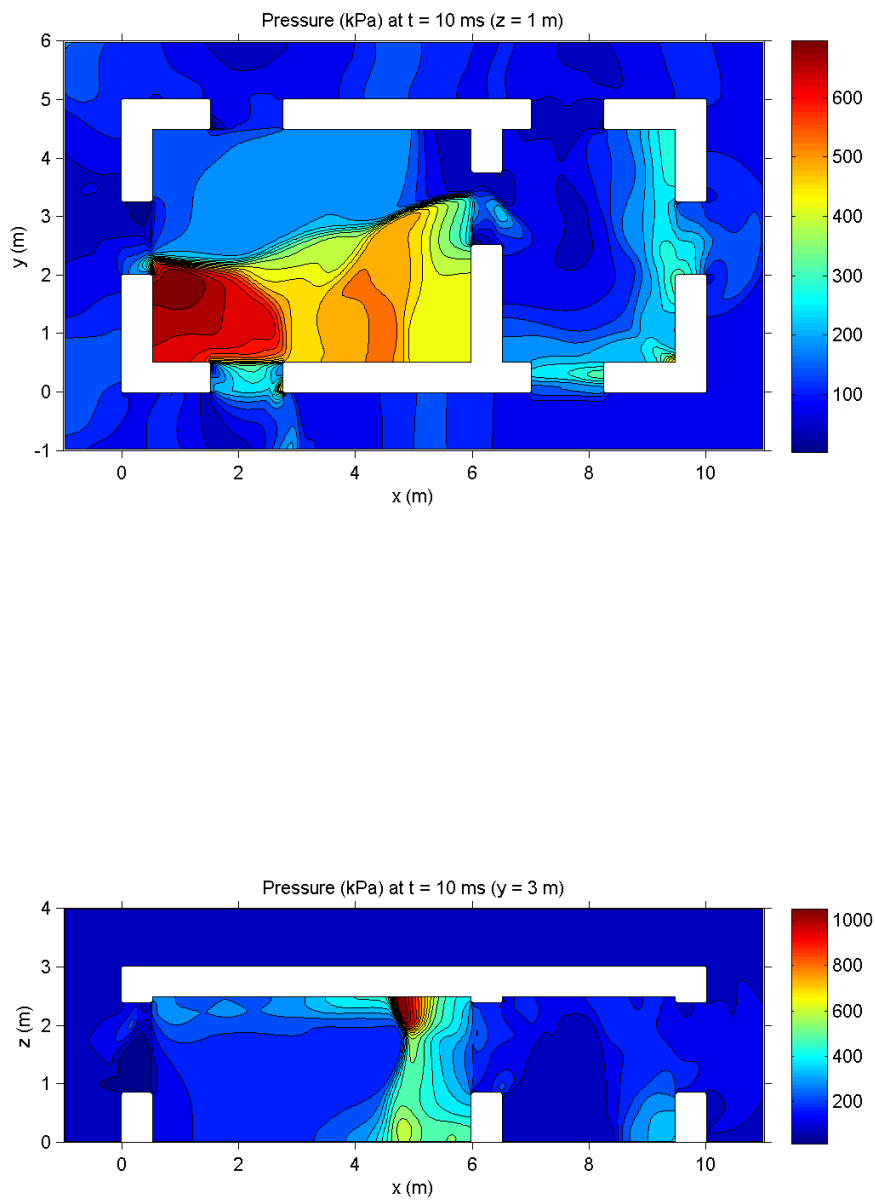
Figure 15: Pressure contours in the horizontal and vertical cross-sections at $t = 10\,\mathrm{ms}$.

DEFENCE SCIENCE AND TECHNOLOGY ORGANISATION DOCUMENT CONTROL DATA		1. CAVEAT/PRIVACY MARKING

2. TITLE	3. SECURITY CLASSIFICATION		
An Accumulated Damage Model for Blast Propagation in Compartmented Structures with Progressively Failing Thin Bulkheads	Document	(U)	
	Title	(U)	
	Abstract	(U)	

4. AUTHOR	5. CORPORATE AUTHOR
L. K. Antanovskii	Defence Science and Technology Organisation PO Box 1500 Edinburgh, South Australia 5111, Australia

6a. DSTO NUMBER	6b. AR NUMBER	6c. TYPE OF REPORT	7. DOCUMENT DATE
DSTO–TR–2365	AR-014-673	Technical Report	December, 2009

8. FILE NUMBER	9. TASK NUMBER	10. SPONSOR	11. No OF PAGES	12. No OF REFS
2008/1132306/1	NS 07/002		17	27

13. URL OF ELECTRONIC VERSION	14. RELEASE AUTHORITY
http://www.dsto.defence.gov.au/corporate/ reports/DSTO–TR–2365.pdf	Chief, Weapons Systems Division

15. SECONDARY RELEASE STATEMENT OF THIS DOCUMENT
Approved For Public Release

OVERSEAS ENQUIRIES OUTSIDE STATED LIMITATIONS SHOULD BE REFERRED THROUGH DOCUMENT EXCHANGE, PO BOX 1500, EDINBURGH, SOUTH AUSTRALIA 5111

16. DELIBERATE ANNOUNCEMENT
No Limitations

17. CITATION IN OTHER DOCUMENTS
No Limitations

18. DSTO RESEARCH LIBRARY THESAURUS	
Science	Mathematical modelling
Physics	Blast loads on structures
Vulnerability	Damage accumulation
Lethality	Failure probability

19. ABSTRACT

This report addresses the development of a model for blast propagation in compartmented structures with progressively failing thin structural elements like windows. The mathematical model is based on the assumption that the frangible structural features (a) are thin compared to the characteristic length scale, (b) do not deform much before breakage, and (c) fail instantaneously when the corresponding accumulated damage reaches some threshold. The presented numerical model employs a variation of the Godunov scheme for blast propagation, coupled with a simple governing equation for the accumulated damage of finite elements constituting a structural feature with empirical coefficients estimated from the pressure-impulse diagram. When the accumulated damage exceeds some threshold value, a group of finite elements representing a designated entity like a single window, is forced to fail thus instantaneously changing the computational domain topology. The illustrative numerical simulations in three dimensions demonstrate that the model behaves reasonably well and is capable of providing rough estimates of progressive failure and blast transfer within and between compartmented structures.